https://doi.org/10.5194/egusphere-2024-1435
Preprint. Discussion started: 10 June 2024

Disentangling the drivers behind the post-2000 retreat of Sermeq Kujalleq, Greenland (Jakobshavn Isbrae)

Ziad Rashed[1], Alexander A. Robel[1], and Hélène Seroussi[2]

[1]School of Earth and Atmospheric Sciences, Georgia Institute of Technology, Atlanta, GA, USA
[2]Thayer School of Engineering, Dartmouth College, Hanover, NH, USA

Correspondence: Ziad Rashed (zrashed3@gatech.edu)

Abstract. Ocean temperatures have warmed in fjords surrounding the Greenland Ice Sheet, which is causing increased melt along their ice fronts, rapid glacier retreat, and contributes to rising global sea levels. However, there are many physical mechanisms which may mediate the glacier response to ocean warming and variability. Warm ocean waters can directly cause melt at horizontal and vertical ice interfaces, or promote iceberg calving by weakening proglacial melange or undercutting the glacier front. Sermeq Kujalleq (also known as Jakobshavn Isbræ) is the largest and fastest glacier in Greenland and has undergone substantial retreat starting in the late 1990s. In this study, we use a large ensemble modeling approach to disentangle the dominant mechanisms driving the retreat of Sermeq Kujalleq. Within this ensemble, we vary the sensitivity of three different glaciological parameters to ocean warming: frontal melt, subshelf melt and a calving stress threshold. Comparing results to the observed retreat behavior from 1985-2018, we select a best-fitting simulation which reproduces the observed retreat well. In this simulation, the arrival of warm water at the front of Sermeq Kujalleq in the late 1990s leads to enhanced rates of subshelf melt, leading to the disintegration of the floating ice tongue over a decade. Retreat into a substantially deeper bed trough around 2010 accelerates retreat, which continues nearly unabated despite local ocean cooling in 2016. An extended ensemble of simulations with varying calving threshold shows evidence of hysteresis in calving rate, which can only be inhibited by a substantial increase in calving stress threshold beyond values suggested for the historical period. Our findings indicate that accurate simulation of rapid calving-driven glacier retreats requires more sophisticated models of iceberg mélange and calving evolution coupled to ice flow models.

1 Introduction

Observations indicate that many glaciers in Greenland have undergone rapid retreat over the last few decades. Sermeq Kujalleq (hereafter SK, also known as Jakobshavn Isbræ) is a fast-flowing marine-terminating glacier in West Greenland, which has been the fastest and largest contributor of Greenland ice discharge for the past several decades (Mouginot et al., 2019). SK has experienced considerable thinning and retreat with terminus velocities almost doubling from ∼6,700 m/yr in 1985 to ∼12,600 m/yr in 2003 (Holland et al., 2008; Joughin et al., 2014). As a result of this mass loss, SK was singularly responsible for 4% of the total 21st century sea level rise. Prior to this rapid acceleration, SK was considerably slower, experiencing moderate thickening from 1991-1997 (Schweinsberg et al., 2017; Joughin et al., 2004). Prior to 2000, SK had a floating ice tongue

https://doi.org/10.5194/egusphere-2024-1435
Preprint. Discussion started: 10 June 2024

providing some stability by buttressing of the terminus (Echelmeyer and Harrison, 1990) and buffering of frontal melt rates. The intrusion of warmer subsurface waters into Disko Bay and the Illulisat Icefjord in the late 1990s preceded collapse of the floating ice tongue (Holland et al., 2008), which is widely thought to have initiated the retreat and acceleration of SK over the next 20 years.

While it is generally agreed that warm subsurface waters triggered the most recent retreat phase of SK (Holland et al., 2008; Myers and Ribergaard, 2013), there is still debate about which physical processes are responsible for mediating the glacier response to ocean warming. The greatest increases in SK's terminus flow speed occurred in the summers of 2012 to 2015 (Khazendar et al., 2019) but initial warming (1-2°C) of Disko Bay fjord waters occurred a decade prior, indicating a lag in SK's flow response to warming ocean conditions. Conversely, SK flow speeds decreased concurrently with the cooling of Disko Bay water by 1.5 °C in 2017. Based on this relationship between glacier speed and fjord temperatures, it has been argued that enhanced melting of the terminus caused greater calving, retreat, and speed-up, particularly in summer when buoyant subglacial meltwater plumes should enhance circulation at the terminus (Khazendar et al., 2019). On the other hand, previous intervals of enhanced fjord heat content prior to the 1980s did not result in the same dramatic retreat (Slater et al., 2018), leading to the natural question: why did the most recent period of warming cause such a dramatic and unprecedented retreat? While water temperatures in Disko Bay are associated with melt and retreat at SK, it is still not clear whether this association indicates a causal relationship between enhanced terminus melt and observed thinning and retreat (Joughin et al., 2020), and whether the recent retreat is the direct result of oceanographic or glaciological factors. Alternatively, the strength of iceberg mélange and undercutting via frontal melt have been observed to have strong control on calving frequency and style at SK and other glaciers (Joughin et al., 2004; Amundson et al., 2010; Cassotto et al., 2015; Luckman et al., 2015; Kajanto et al., 2023). Disentangling the drivers behind SK's response to warming ocean conditions requires distinguishing between retreat driven through direct melting and calving.

Understanding the response of SK to warming ocean waters poses a difficult challenge, owing to the complex range of processes occurring at its interface with the ocean. Many processes that play a critical role in glacier stability (i.e., subshelf melting, calving, melt undercutting, mélange buttressing) remain poorly understood, despite recent advancements in high-fidelity glacier models (Benn et al., 2017; Slater et al., 2021). Furthermore, the process of acquiring the necessary observations to limit the potential values of modeling parameters becomes challenging due to the presence of icebergs in winter seasons. Simplified parameterizations that relate calving rates to glacier stress and geometric conditions are used in many ice sheet models (Benn et al., 2007), but do not always capture the complex interactions between glacier and ocean state. Additionally, parameterizations which may perform well in describing one glacier might not perform as well at other glaciers (Amaral et al., 2020). Here, we use SK's rapid retreat and complex evolution over the past decades as a natural experiment to better understand uncertainties and shortcomings in simple parameterizations of ice-ocean interactions.

In this study, we simulate the historical evolution of SK from 1985 to 2018 using the Ice-Sheet and Sea-Level System Model (Larour et al., 2012). We perform a large ensemble of simulations of SK retreat through perturbation of three sensitivity parameters that impact its retreat: subshelf melt, melt at the calving front, and calving modulated by mélange rigidity. We compare model simulations to the relevant period of the observational record by scoring their ability to reproduce observed

https://doi.org/10.5194/egusphere-2024-1435
Preprint. Discussion started: 10 June 2024

calving front geometry. We investigate the trade-off between different processes in driving SK's temporal and spatial sensitivity to melt- and stress-based mechanisms of mass loss and highlight the possible mechanisms most likely responsible for observed retreat.

In section 2, we lay out the methodology for simulating SK's evolution from 1985-2018. We describe how simulations are initialized in the Ice-Sheet and Sea-Level System Model and the specific data used to recreate the state of SK in 1985. We then explain how melt and calving processes are parameterized with respect to ocean forcing and how we design our ensemble to determine which parameter combination results in model output that most closely matches observational data. In section 3, we present our model ensemble results and highlight key relationships between model parameters that best fit observations. Additionally, we analyze the timing and extent of retreat within the model with the best match to observations. In section 4, we discuss implications for SK's future evolution given its current state. We also discuss how our results compare to previous studies and hypotheses regarding SK's rapid retreat.

2 Methods

2.1 Model Configuration

We use the Ice-Sheet and Sea-Level System Model (ISSM) to simulate the retreat of SK from 1985 to 2018. ISSM is a state-of-the-art thermomechanical ice sheet model that has been used to simulate ice sheet evolution of glacier and at continental scales (Larour et al., 2012). Our modeling approach draws on some aspects of the configuration of a previous SK modeling study by Bondzio et al. (2018), with some key enhancements detailed in this section. The domain of our simulations includes the fast-flowing parts of the SK catchment and extends upstream deep into the SK catchment area. We use a mesh with a horizontal resolution which ranges from 400 m near the grounding line to 7 km at the most upstream parts of the catchment. A 2D shelfy-stream approximation (SSA; Morland and Zainuddin, 1987; MacAyeal, 1989) is used to simplify the three-dimensional flow equations as vertical gradients in velocity are relatively small and basal sliding is the dominant contributor to ice velocity at SK. The SSA approximation greatly reduces the computational expense of simulating marine-terminating glacier evolution and thus enables the large ensembles of simulations in this study. A linear-viscous sliding relation (Budd et al., 1984) is used and appropriate sliding coefficients were inverted by using composite velocities collected in 1991 and 2009 for the area close to the ice front (Rignot and Mouginot, 2012), which have been scaled down to give a smooth transition between both data sets. A sub-element migration scheme allows the simulated grounding line to evolve continuously through mesh elements and limit the dependence on mesh resolution (Seroussi et al., 2014). At the upstream boundary of the domain, ice velocities are set to observed ice velocities and the corresponding ice thicknesses are kept constant. The model time step is approximately 5.5 hours in order to capture rapid changes in ice terminus geometry while maintaining numerical stability and accuracy. We use a spatially variable surface mass balance held constant in time, based on a multidecadal mean from the RACMO regional climate model (Ettema et al., 2009). While SMB over our region of interest changed over the time period considered, the magnitude of its variability relative to the time average is much smaller than that of oceanic forcings (Hanna et al., 2011). Additionally, it has been shown that the SK region is weakly sensitive to atmospheric forcings within our time period of interest (Seroussi et al.,

https://doi.org/10.5194/egusphere-2024-1435
Preprint. Discussion started: 10 June 2024

2013) and we can consider atmospheric forcings to be more influential in it's role modulating ocean conditions. We initialize simulations with 1985 ice surface topography obtained via photogrammetry (Korsgaard et al., 2016) with gaps filled using the Greenland Ice Mapping Project (Howat et al., 2014) and corrected with an offset proportional to the ice flow velocity. Bedrock topography used in these simulations is from BedMachine Greenland v3 (Morlighem et al., 2017).

Migration of the calving front is simulated using a level set formulation (Bondzio et al., 2016), where the migration rate of the calving front ($\boldsymbol{w}$) is determined using the difference between ice velocity and frontal ablation rate,

$$\boldsymbol{w} = \boldsymbol{v} - (c + m_{\mathrm{fr}})\,\boldsymbol{n} \tag{1}$$

where $\boldsymbol{v}$ is the ice velocity at the calving front, and $c + m_{\mathrm{fr}}$ is the ablation rate. Ablation at the calving front is driven by two parameterized processes: iceberg calving (c is calving rate) and direct melt of the calving front by heat flux from the ocean (m_{fr} is frontal melt rate). In the level set approach, ice flow advects the calving front downstream and ablation mechanisms move the calving front upstream.

2.2 Stress-based iceberg calving threshold

Iceberg calving rate is calculated with a tensile-stress based criterion (inspired by criteria based on the von-Mises principal tensile stress)

$$c = |\boldsymbol{v}|\frac{\sigma}{\sigma_{\mathrm{thr}}}, \tag{2}$$

where σ is the principal tensile stress, σ_{thr} is a prescribed stress threshold, and $\boldsymbol{v}$ is the ice velocity magnitude at the ice front (Morlighem et al., 2016).

Calving-induced retreat of the glacier front is initiated once local principal tensile stresses exceed the stress threshold parameter (σ_{thr}). The stress threshold parameter can be thought to conceptually represent many physical processes that have the ability to modify the propensity for calving events. We parameterize a linear decrease in calving threshold, σ_{thr}, with increasing fjord ocean temperatures ($\boldsymbol{T}$)

$$\sigma_{\mathrm{thr}} = \sigma_{\mathrm{max}} - \frac{\boldsymbol{T} - \min(\boldsymbol{T})}{\max(\boldsymbol{T}) - \min(\boldsymbol{T})}(\sigma_{\mathrm{max}} - \sigma_{\mathrm{min}}). \tag{3}$$

The minimum stress threshold corresponds to the warmest temperature in the fjord temperature time series, and conversely the maximum stress threshold corresponds to the coldest temperature in the fjord temperature time series. Due to the fractured nature of near-terminus ice at SK, we set this minimum calving stress threshold to 100 kPa, below the measured mechanical strength properties of laboratory samples of pristine ice, typically in the range of 0.1-1 MPa (Lee and Schulson, 1988; Petrovic, 2003). The temperature dependence of the stress threshold ensures that calving activity increases when the ocean in contact with the glacier is warmer. This stress threshold is intended to parameterize the potential roles of iceberg mélange and melt undercutting in modulating the relationship between fjord ocean temperatures and calving rate. Though other material properties and glacier processes may play a role in setting the propensity for calving (e.g., fracture toughness of ice, surface melt), they

https://doi.org/10.5194/egusphere-2024-1435
Preprint. Discussion started: 10 June 2024

are not able to explain the timing of seasonal and multi-annual changes in calving style at SK (Joughin et al., 2008). In section 4, we further discuss the shortcomings of such a simplified representation of the effect of mélange on calving.

2.3 Frontal and submarine melt

Ocean melt of the glacier calving front (referred to hereafter as frontal melt) also contributes to the glacier response to fjord temperatures. We compute the frontal melt rates using the empirical parameterization from Rignot et al. (2016); Xu et al. (2013):

$$m_{\mathrm{fr}} = (A\ h\ {Q_{\mathrm{sg}}}^{\alpha} + B)\ T^{\beta}, \tag{4}$$

where Q_{sg} is the subglacial discharge which is taken as the total runoff of SK's drainage basin as given by RACMO 2.3 (Noël et al., 2015), T is the ocean thermal forcing obtained via the depth-integrated temperature of the water column near the glacier front, and h is the depth of the water column. This empirical equation has been shown to be a good approximation of how frontal melt relates to ocean temperature and subglacial discharge at some glaciers in Greenland, based on in-situ observations and numerical simulations (Rignot et al., 2016). Since Q_{sg} and α are sufficiently small, and β is sufficiently close to one, we assume that frontal melt is linearly proportional to thermal forcing to simplify the following analysis.

Submarine melt on the floating portion of the glacier is the final process we consider contributing to the glacier response to fjord temperatures. The submarine melting rate is computed using the simplified two-equation parameterization from Holland and Jenkins (1999)

$$m_{\mathrm{sm}} = -\rho_M c_{pM} \gamma_T (T - T_{pmp}). \tag{5}$$

where ρ_M is the mixed layer density, c_{pM} is the specific heat capacity of the mixed layer, γ_T is the thermal exchange velocity, and $(T - T_{pmp})$ is the difference between the mixed layer and the pressure melting point temperature at the base of the ice.

2.4 Model-Observation Mismatch Score

We choose a parameter space for multipliers of forcing mechanisms such that we encompass a large range of possible forcing scenarios. For our frontal and submarine melt parameters space, we choose a range of 0-4x the empirical parameterizations mentioned in equations (5) and (4). We choose to plot results for max stress threshold varying over 220-360kPa with an interval of 10 kPa to ensure we capture both potentially rigorous and negligible calving activity. We also conducted additional simulations outside the aforementioned parameter bounds, particularly with a much wider range of calving stress threshold. But, simulations with prescribed stress thresholds outside the bounds plotted in the next section produced retreats (or lack of retreat) very different from those observed in reality. Thus, we opted not to plot those here. Each simulation is scored based on its correspondence to the observed position and geometry of the glacier calving front. We use a historical catalog of SK's calving front geometry (i.e., a 2-D curve) obtained from observational records which includes multiple snapshots of calving

https://doi.org/10.5194/egusphere-2024-1435
Preprint. Discussion started: 10 June 2024

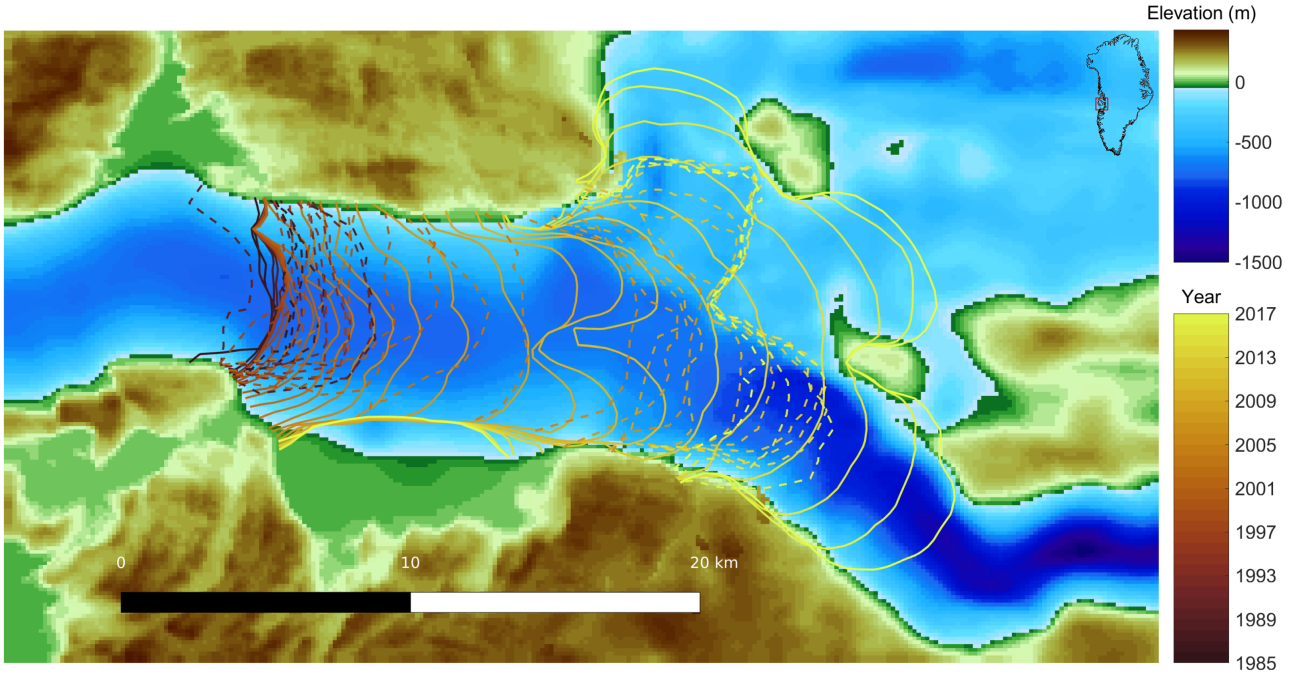

Figure 1. Observed and simulated calving fronts from our highest scoring simulation at SK from 1985-2018. Thicker lines denote outputs from our best fitting ensemble member. The dashed lines indicate the observed positions of SK's calving front with the color corresponding to the year of observation.

front geometry derived from Landsat 5–8, ERS-1 and 2, and TerraSAR-X satellite imagery (Figure 1). We pair each observed terminus geometry with the nearest-in-time (always within less than 5 days) modeled terminus geometry from ISSM. For each observation-model pair, we calculate the area between the modeled and observed terminus geometry. Though we do not weight scores to account for changing observational density in time, almost all of the retreat of SK occurs during a time period (post-2000) when observational density is high. Thus, the mismatch score is unlikely to be strongly dependent on observational density. Using this scoring method, we can accurately capture changes in calving front position and shape and are only limited by the resolution of the observational records and model meshing. Convergence studies indicate that at our chosen model time step, potential errors due to the mismatch in timing between model and observation contribute negligibly to the overall scored metric. For every ensemble member, we take the root mean square of the error vector as the overall score for the simulation to measure how well the model did in matching calving front geometry. This is different from the approach of Bondzio et al. (2018) which only considers the center line position of the SK calving front, as considering the entire calving front geometry allows for more accurate tracking of the glacier when the front bifurcates, as it did in 2006.

https://doi.org/10.5194/egusphere-2024-1435
Preprint. Discussion started: 10 June 2024

3 Results

The speed and timing of the simulated retreat of SK vary depending on the sensitivities of calving threshold, submarine melt, and (to a lesser extent, discussed below) frontal melt to local ocean temperature, but there are some commonalities between simulations in our perturbed-parameter ensemble. Figure 1 shows the observed calving front positions (thin lines) and the results of one simulation with the best correspondence to observations (thick lines). Generally, the calving front of SK pauses at locations where there are geometric pinning points such as bedrock peaks and fjord narrowings. However, the length of time that the simulated glacier remains at such pinning points varies, due to the interplay of calving and melting. Initially, the ice tongue of SK stabilized the glacier front by buttressing inland ice. As in observations (Motyka et al., 2011), simulations generally indicate that intensified submarine melting due to warming of fjord waters starting around 1997 thinned the ice tongue and weakened its buttressing capacity. The weakening and subsequent disintegration of SK's ice tongue result in dynamic thinning of the terminus and an acceleration in retreat. Most of the simulations in our perturbed parameter ensemble yield submarine melting rates which peak between 1995 and 2000, as warm water entered Illulisat Icefjord via Disko Bay. The simulated disintegration of the ice tongue and subsequent front retreat leads to the bifurcation of the calving front into two branches and exposure of a much larger frontal area to warm ocean waters. The response of SK's branches is not homogeneous owing to large differences in their bed topography and fjord geometry. Ice fluxes are greatest along the southern calving front where the bedrock is deeper and upstream topography is characterized by more extensive retrograde slopes. The combination of a thicker and steeper glacial terminus and deepening grounding line bed slopes facilitate ice loss via calving. Thicker ice results in a greater overburden pressure which, at the grounding line, is counterbalanced by hydrostatic pressure and buttressing stresses from floating ice and mélange. Thus, following the removal of the ice tongue, tensile stresses grow rapidly along the southern front and calving quickly becomes the dominant ice loss mechanism. The northern branch of SK experiences much less retreat, similarly to what observations show. The shallow bed topography and an abundance of pinning points constrain the upper branch from rapidly retreating following the ice tongue disintegration. Tensile stresses along the upper branch's calving front grow but do not result in rapid calving as observed in the lower or main branch.

3.1 Perturbed-parameter ensemble of SK retreat simulations

In our large perturbed-parameter ensemble, multiple simulations were able to achieve nearly equivalent matches to the observed retreat of SK (Figure 2). There appears to be a minimum achievable match to observations (with RMSE of approximately 40 km^2) related to observed changes in calving style unrelated to ocean temperatures, which we discuss in more detail in section 4. We also expanded our ensemble extent within parameter space beyond the ranges plotted in Figure 2 to verify that the best fitting simulation was indeed the best fit. The best scoring simulations all occur within a similar region of parameter space, plotted in Figure 2. Outside of this region of parameter space, model-observation mismatch scores are consistently much worse. The cold-ocean maximum of calving stress threshold in this region of parameter space is 250-400 kPa, generally much lower than suggested by laboratory studies, and near the low end of the range of observationally derived values for fractured glacier fronts (Vaughan, 1993; Choi et al., 2018).

https://doi.org/10.5194/egusphere-2024-1435
Preprint. Discussion started: 10 June 2024

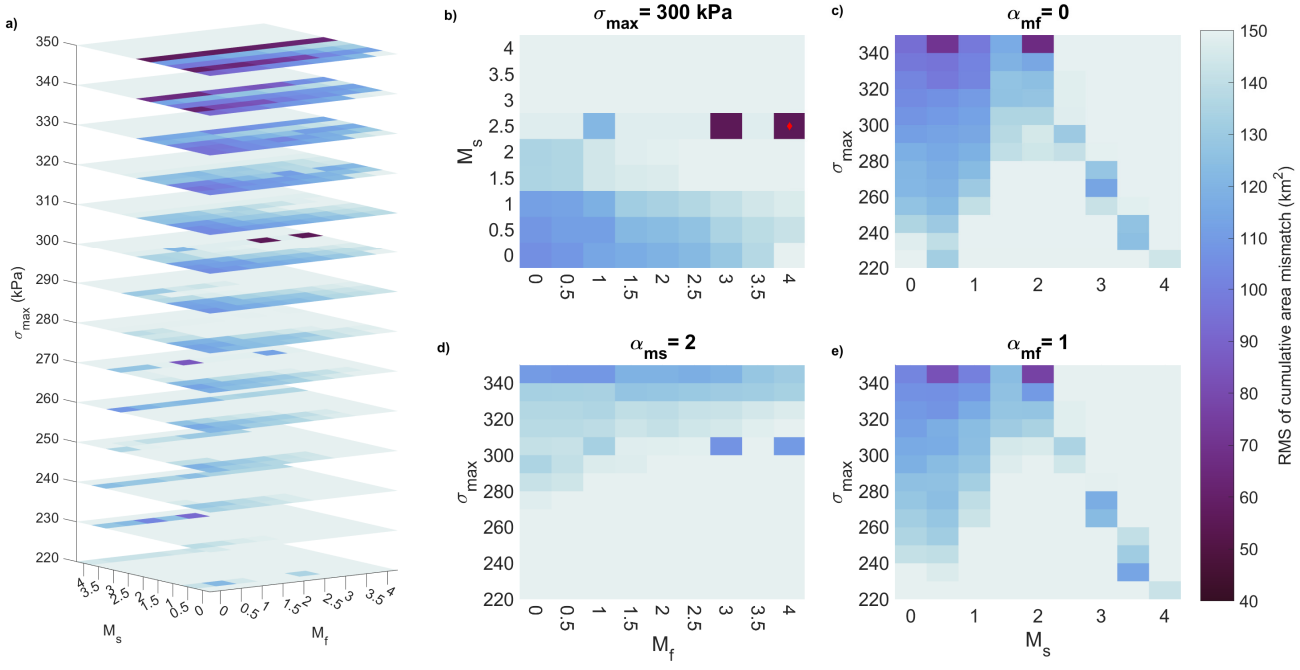

Figure 2. Parameter combination sweep of relevant melt values. Darker colors indicate a smaller RMS error between modeled and observational records of SK's calving front position. Panel a displays the RMS of cumulative area mismatch for specified maximum stress levels. Panels b-d show respective RMS slices for $\sigma_{\max} = 300$kPa, $\alpha_{\mathrm{mf}} = 0$, $\alpha_{\mathrm{ms}} = 2$, and $\alpha_{\mathrm{mf}} = 1$.

The simulations best matching observations generally require submarine melt to be more sensitively dependent on ocean temperatures ($M_s > 1$) than suggested by the two-equation parameterization. However, there is a notable trade-off between the stress threshold and submarine melt, such that simulations with higher cold-ocean stress thresholds (i.e., less calving in cold waters) also need higher submarine melt rates to compensate. Diminished calving of the ice tongue needs to be compensated by amplified submarine melt in order to accurately simulate the timing of ice tongue collapse. The greatest mismatch between models occurs following the collapse of the ice tongue, coinciding with the onset of calving-dominated retreat.

Though the absolute best-fitting simulation requires high sensitivities of front melting to ocean temperatures ($M_f = 4$), there are several simulations with very similar RMSE requiring little to no front melt at all to fit observations. In these simulations, the greatest mismatch occurs following ice tongue collapse which is when calving becomes the dominant mode of ice loss. It is also by this point that thermal forcing from warmer waters contributes less to SK's dynamic response. If the stress threshold is sufficiently low, retreat following ice tongue collapse is controlled by bed topography and ice flux is dominated by calving in the southern trunk. Conversely, retreat is controlled by submarine melt when stress thresholds are considerably larger than tensile stresses generated at the glacier front. Changing frontal melt rates predicted by the Rignot et al. (2016) parameterization by modifying M_f did not significantly change model behavior, nor improve our best fit parameter combination. The weak

https://doi.org/10.5194/egusphere-2024-1435
Preprint. Discussion started: 10 June 2024

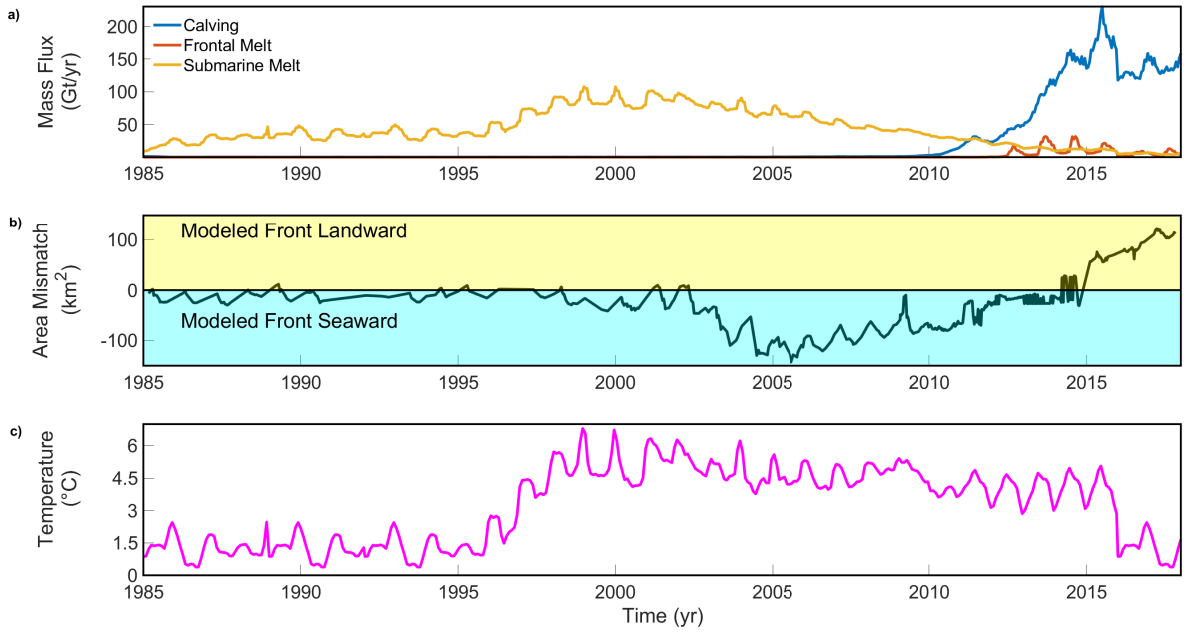

Figure 3. Best fitting model flux contribution and performance. (Top Panel, a) Mass flux contribution of relevant ablation mechanisms to the evolution of SK's calving front. (Middle Panel, b) Difference between modeled and observed calving front areas. (Bottom Panel, c) Estimated Disko Bay fjord temperatures sourced from ECCO2.

dependence of RMSE in Figure 2 to the sensitivity of frontal melt to ocean temperature indicate that, at least for SK, calving and submarine melt control the speed and timing of glacier retreat.

3.2 Best-match simulation

The simulation best fitting observations captures the observed SK calving front geometry well, though there do remain some periods of mismatch. In Figure 3, the fluxes contributing to ice loss at the calving front are decomposed (panel a), along with the fit to observations (panel b), and the ocean forcing from the ECCO2 reanalysis product (panel c).

During the period from 1985 to 2000, SK maintained a floating ice tongue ahead of its terminus. While the floating ice tongue existed, observed surface ice flow velocities exhibited very little seasonal variability (Echelmeyer and Harrison, 1990) indicating a glaciological state in which dynamic thinning due to ocean melt is consistently balanced by surface accumulation and ice flow from upstream. SK's ice tongue acted as buffer for retreat through two primary mechanisms: (1) transmitting buttressing back stress from the Illulisat Icefjord walls to the grounding line, and (2) acting as a heat sink for warm ocean waters. Local ocean temperatures experienced an abrupt increase in 1997, which led to the disintegration of SK's ice tongue over several years and the subsequent thinning and accelerated retreat of the newly exposed terminus.

https://doi.org/10.5194/egusphere-2024-1435
Preprint. Discussion started: 10 June 2024

In our best-fitting simulation, the rise in ocean temperature causes an increase in submarine melt fluxes, which is then followed by the simulated ice tongue thinning and retreat. Submarine melt initially dominates ice loss, peaking as ocean temperatures reach their maximum in 2000. Following this peak, submarine melt fluxes slowly decrease albeit at a rate faster than ocean temperatures decrease due to the decreasing area of the floating ice tongue. During this period, the base of the ice tongue steepens, which causes a subsequent rise in driving stress and extensional stresses, which promotes calving activity. However, we do not see a corresponding increase in calving fluxes immediately following the temperature increase. This is most likely due to the response timescale associated with the geometric adjustment of the floating ice tongue and corresponding stress state of the terminus, which depends more on the instantaneous glaciological state rather than the oceanic state. It should also be noted that during this period of retreat, SK's front is still far enough downstream that it has not begun retreating via its two branches. This is important because this part of Illulisat Icefjord has a slight prograde bed slope. Thus, this period is marked by a relatively slow retreat driven by submarine melt, which sets up the glacier for further retreat as persistently warm water continues to force the glacier front.

During the period from 2000-2012, SK's retreat begins to accelerate. In this phase of the retreat, the change in SK's geometry begins to play an important role in setting the calving rate at the terminus. In this period, we also mark a point at which the dominant mechanism of retreat transitions from melt-dominated to calving-dominated, with melt accounting for a greater ice flux at the beginning of the period and calving at the end of the period. This transition is caused by the recession of the grounding line into a deeper bed and a final removal of the last part of the floating ice tongue. From 2000-2005, there is a decrease in submarine melt flux caused mostly by the reduction in floating ice tongue area, and to a lesser extent the relative decrease in ocean temperature forcing. By 2005, SK's calving front has retreated enough to lie across the upper and lower branches, which introduced a greater variability in bed topography along the front. The greatest sustained discrepancy between modeled and observed glacier geometries occurs over the 2005-2010 period, as our modeled terminus lags downstream of the observed terminus. The mismatch in geometry is largely amplified by the differences in calving rate as there is a trade-off between capturing accurate calving rates after 2010 and insuring minimal mismatch between 2005 and 2010 as the dominant mode of ice loss changes. During this period, we observe the transition to a calving-dominated retreat owing to geometric changes at the calving front. The combination of a retrograde bed and a steep ice cliff front geometry promotes intensified calving activity along the lower branch of SK. By 2010, SK's ice tongue has been completely removed and the calving front is a steep ice cliff. The time at which model ensemble members reach this transition point would be the greatest source of variability in overall error between modeled and observed calving fronts.

By 2010, the model simulates a rapid acceleration in calving rate and a better fit between modeled and observed calving fronts. From 2010-2016, calving fluxes increase and SK's front retreats considerably more along its lower branch than its upper branch. The transition of SK to a calving-dominated retreat after 2010, and the lack of substantial re-advance during the brief cooling between 2016-2018 raise the possibility that the SK has undergone a hysteretic change to irreversible calving-dominated retreat (discussed further in the next section). Other studies have also raised this possibility. Due to the strong topographical control on retreat rate, we expect that once the lower branch's grounding line retreats past the over-deepened

https://doi.org/10.5194/egusphere-2024-1435
Preprint. Discussion started: 10 June 2024

trough, a rapid acceleration of retreat is very likely regardless of climate forcing Kajanto et al. (2020). This retreat is largely driven by calving fluxes as floating ice area considerably decreases and the effects of submarine melting are diminished.

3.3 Potential hysteresis effects of ice mélange

In our best-fitting simulations, calving rate at SK rapidly accelerates in concert with retreat into a deep trough on the southern flank of the glacier catchment. The glacier bed in this trough further deepens over 20-30 km upstream of the 2018 calving front position, raising the spectre of hysteresis to permanently high calving rates, regardless of future climate forcing. However, other studies have raised the possibility that increased calving will produce a thicker ice mélange which could inhibit calving. As described in section 2, our simulations do not account for this potential negative feedback, assuming that calving rate is only sensitive to ocean temperatures and glacier front geometry.

To simulate the potential for hysteresis effects associated with calving, we continue the best-matching simulation from the large ensemble described in the previous section in a series of simulations with an increased calving stress threshold until 2100. Figure 4 shows that the resulting simulations exhibit two types of behavior. When the calving stress threshold is held at 260 kPa, the value given by the best fitting simulation in 2018, calving rate continues to increase peaking around 2050 at rates more then twice 2018 rates. This behavior is shared with a grouping of ensemble members (260-437 kPa) and consistently results in an almost complete retreat into the ice sheet interior by 2100. Ensemble members with a stress threshold above 437 kPa stabilize, but do not readvance. In these simulations, the calving front stabilized in the deepest trough along the flowline and the glacier experienced gradual thickening. We note here that such calving stress thresholds were not attained at any point during the historical time period used to calibrate the stress threshold (i.e., they are above the cold-ocean σ_{max}found for all best-fitting simulations in the parameter sweep described in the previous section. Thus, even if ocean temperatures returned to the coldest values achieved during the historical period over the next 80 years, the rapid acceleration of calving and retreat would likely continue unabated.

4 Discussion

In this study, we have investigated the drivers behind SK's recent retreat from 1985-2018. By considering only processes related to ocean forcing, we are able to closely reproduce the observed evolution of SK and analyze the mechanisms responsible for its retreat before and after ice tongue collapse. Our best-fitting model simulations match those sparse observations which do exist, but also allow us to understand the physical mechanisms that drove the observed retreat in a physically self-consistent manner. Thus, we can paint a fuller picture of the dynamics responsible for SK's evolution.

We noted two distinct behaviors in glacier evolution in the simulations plotted in Figure 4, extending past 2018. The first is arrest of the calving front retreat on a prograde slope following rapid retreat. The second is characterized by a rapidly accelerating retreat which extends 10's of km into SK's interior followed by arrest of retreat. The location at which arrest or rapid retreat occurs is consistent across these simulations. However, the timing of rapid retreat and arrest varies marginally between ensemble members. This further reinforces the notion that SK's current retreat is controlled by bed topography, with

https://doi.org/10.5194/egusphere-2024-1435
Preprint. Discussion started: 10 June 2024

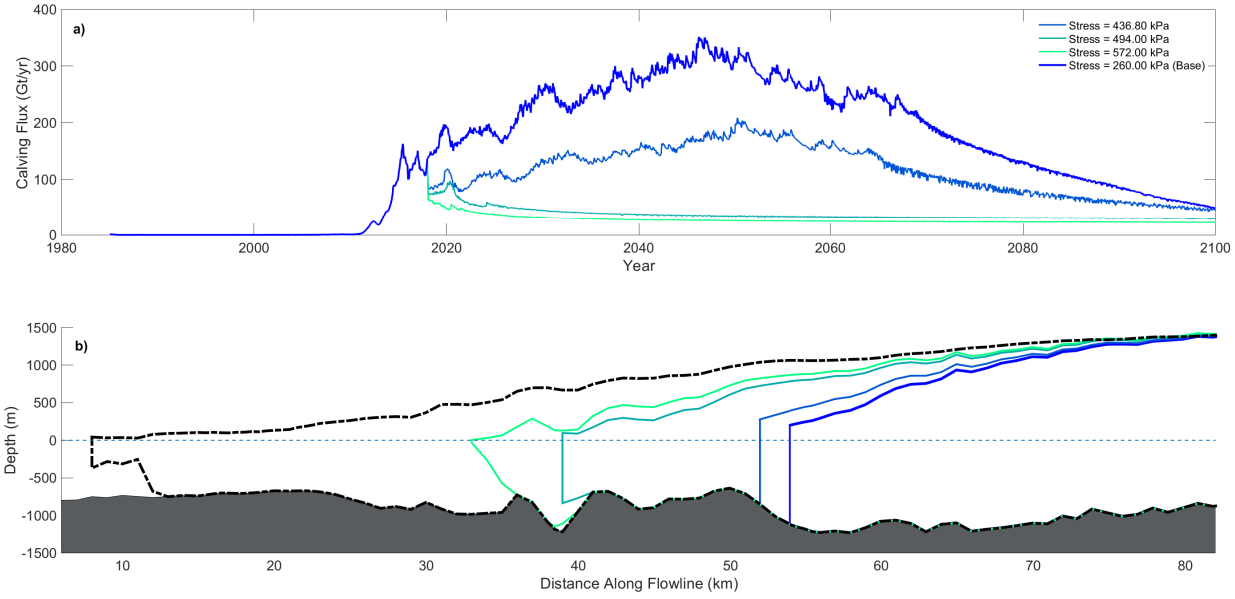

Figure 4. Top Panel (a): Calving fluxes of 2100 run ensemble members from 1985 to 2100 with the onset of stress amplification at 2018. Bottom Panel (b): Along flowline profiles of ensemble members at year 2030. The initial 2018 profile is denoted with a thick black dashed outline and sea level is denoted with a blue dashed line.

the stress threshold (and all the factors which determine it) influencing the amount of time it takes to reach the rapidly calving state. This behavior is indicative of threshold behavior, wherein a small change in a parameter (in this case calving stress threshold) will lead to either a stable and slightly advancing SK or a rapidly retreating and unstable SK.

In designing simulations that can be used to disentangle the drivers of SK retreat, certain simplifications were necessary which limit the broad applicability of this study. In order to assess the main drivers behind SK's retreat, certain assumptions were made in our simulations. We do not simulate higher order approximations for the glacier momentum balance (i.e., Full Stokes). We instead rely on the SSA in order to reduce computational expense, enabling a large ensemble of simulations, while maintaining an accurate representation of grounding line dynamics. A direct consequence of simplifying the flow equations is the overestimation of the basal drag coefficient near the grounding line (Morlighem et al., 2010). Bondzio et al. (2017) showed that the basal sliding law and coefficients captured SK's behavior fairly well.

Calibrating multiple model parameters (in this case M_f, M_s and σ_{max}) allows us to produce simulations which fit observed retreat of SK reasonably well. In Bondzio et al. (2018)'s study, a novel large ensemble approach was used to forecast SK's behavior under an collection of parameter combinations of M_f, M_s and σ_{max} which were held constant in time. We expanded on this work by using a similar methodology to discern which mechanisms were most responsible for initiating and maintaining SK's retreat. We find that dynamically adjusting calving propensity via mélange's control on σ_{max} yields modeled calving

https://doi.org/10.5194/egusphere-2024-1435
Preprint. Discussion started: 10 June 2024

fronts which closely match observed calving fronts without requiring melt forcing to be multiple factors larger than observed. These historical simulations enabled us to better understand the factors which drove SK's retreat. However, ultimately such an approach is limited in its ability to explain the role of physical processes not included in our modeling system and how they may evolve outside of the historical sample of satellite observations of SK. The extended simulations described in section 3.3 indicate that the only way to arrest the future retreat of SK is by increasing the calving threshold to values never attained during the historical period and not achievable by changes in ocean temperature alone. We do recognize that it is possible that SK is engaged in runaway retreat that will not be arrested by any mechanism in the next century. But, to even allow for the possibility that SK retreat could slow down or arrest in the future, other processes which play a role in modulating calving must be simulated. Given SK's potential to generate large and dense ice mélange fields, this suggests that a strong enough ice mélange, potentially generated through vigorous calving, may be able to suppress runaway calving behavior. Simulating such a feedback would require a dynamic model of ice mélange coupled to the ice sheet and the ocean below. No mélange model currently exists which fits these requirements, though prior efforts have produced useful parameterizations (Vaňková and Holland, 2017; Pollard et al., 2018; Amundson and Burton, 2018; Schlemm and Levermann, 2021) and very computationally expense tools unfit for coupling to ice sheet models (Robel, 2017; Burton et al., 2018). However, our study indicates that a fully capable and coupled model of mélange is a pre-requisite for any attempts to accurately model SK's future evolution.

5 Conclusions

In this study, we conducted numerical simulations of Sermeq Kujalleq using ISSM to disentangle the relative importance of different mechanisms in driving the retreat of SK from 1985-2017. Using a large ensemble of parameter-perturbed simulations, we explored a wide parameter space of calving and ocean melt parameterizations and compared calving front positions to key observations to score a given simulation on how well it could match observations of retreat. We found that submarine melting and calving both played critical roles in the timing and magnitude of SK's retreat. Specifically, we note that intensified submarine melting due to anomalous deep water temperatures was necessary to instigate rapid retreat by melting SK's ice tongue. Following the loss of the ice tongue, calving became the dominant mechanism of retreat, owing to the exposure of a tall calving front with correspondingly high stresses exceeding the calving threshold. Calving rates rapidly increased as SK retreated into deeper waters and therefore experienced greater tensile stresses along its calving front. The best-fitting simulations display the largest discrepancies with observations during periods of rapid retreat or periods of transition between dominant ablation modes.

Additionally, throughout our model space, a bimodality in calving front positions by 2018 occurs. As seen in Figure 5 there exits two states of final calving front positions. On one end, there exists the set of simulations which do not experience ice tongue loss and subsequently do not experience rapid calving ablation. These simulations are characterized by either lower calving stress thresholds or melting multipliers. While calving front locations are more sensitive to calving thresholds, an insufficiently powerful melting regime is unable to generate a rapid enough removal of the ice tongue which would eventually cascade into the growth of mechanical imbalances at the calving front and subsequent retreat. Within these simulations, the

https://doi.org/10.5194/egusphere-2024-1435
Preprint. Discussion started: 10 June 2024

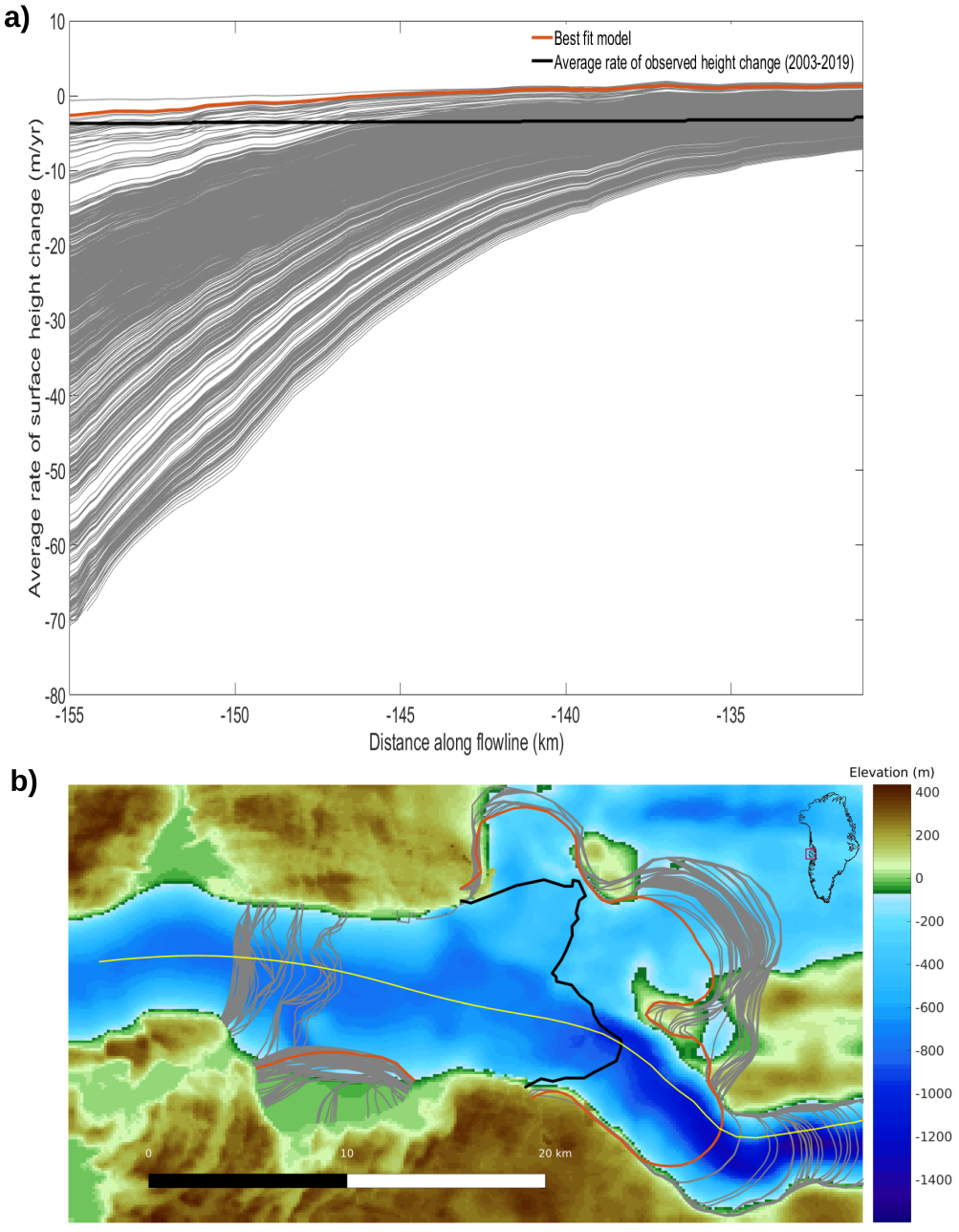

Figure 5. Top panel (a) depicts the average rate of surface height change for all ensemble members along a flowline (denoted in(b)) along the southern SK branch. The average rate of observed height change is obtained from ICESat and ICESat-2 data from 2003-2019 (Smith et al., 2020). Bottom panel (b) displays the 2018 calving front positions for all ensemble members. Additionally the best fit model calving front is highlighted with a dark orange and the observed 2019 winter calving front Smith et al. (2020) with black. The thin yellow line indicates the flowline on which we calculate surface height change.

https://doi.org/10.5194/egusphere-2024-1435
Preprint. Discussion started: 10 June 2024

calving front is quickly arrested and remains quasi-stable. On the other end we see simulations which quickly lose their ice tongue and subsequently accelerate beyond observational records. In this set of simulations, the calving stress threshold plays a greater role than melting in setting the rate of retreat as the grounding line recedes onto deeper bedrock and the glacier front experiences greater mechanical stresses. When letting these simulations continue beyond 2018, we note that rapid calving continues along the southern trunk of SK, but stops across the northern trunk, owing to the presence or lack of steepening bedrock gradients, respectively. Interestingly, we do not witness simulations with calving fronts arresting along a position between the observed calving front in 2018 and a few kms inland from the initial calving front in 1985. The most likely reason for this lies in our simplified parameterization of a dynamic ice mélange. In the absence of mélange, the gross behavior of the SK calving front as modeled here can either be characterized by rapid and vigorous retreat or terminal stability. This leads to a bimodality in model response, while, in reality, ice mélange acts as a stress buffer in response to rapid calving events.

A central finding of this study is that the ability of ice mélange to buttress SK's calving front is increasing in importance as its calving front rapidly retreats onto deeper beds. By extending simulations until 2100 we analyzed the potential for ice mélange to arrest further retreat of SK. Our simulations reveal that a sufficiently robust ice mélange is able to suppress calving activity during SK's most vigorous calving phases. The loss of SK's ice tongue subjected the calving front to greater tensile stress which consequently amplified the importance of ice mélange importance in modulating calving rates. A weakening of ice mélange is likely to have occurred in response to the influx of warm waters into Illulisat Icefjord, which melted integral ice bonds and facilitated downstream movement and fragmentation. This finding emphasizes the importance of future development of dynamic models of ice mélange evolution that can be coupled to ice sheet models.

Code availability. Relevant run and analysis scripts required to produce results found at a persistent Zenodo repository located at https://doi.org/10.5281/zenodo.11176342.

Author contributions. All author help conceive the study and contributed to the manuscript. ZR conducted model simulations, post-processing and analysis.

Competing interests. The contact author has declared that none of the authors has any competing interests.

Acknowledgements. Thanks to Blake Castleman for early work on simulations, and Johannes Bondzio for answering questions on ISSM configuration. Vincent Verjans and John Christian provided useful comments during the completion of this work. This research and authors were supported by funding from a JPL Strategic University Research Partnership (SURP) SP20007. Z. Rashed and A. Robel were also supported by NSF OPP Grant 2025692. H. Seroussi was also supported by NSF NNA Grant 2127246.

https://doi.org/10.5194/egusphere-2024-1435
Preprint. Discussion started: 10 June 2024

References

Amaral, T., Bartholomaus, T. C., and Enderlin, E. M.: Evaluation of iceberg calving models against observations from Greenland outlet glaciers, Journal of Geophysical Research: Earth Surface, 125, e2019JF005 444, 2020.

Amundson, J. M. and Burton, J.: Quasi-static granular flow of ice mélange, Journal of Geophysical Research: Earth Surface, 123, 2243–2257, 2018.

Amundson, J. M., Fahnestock, M., Truffer, M., Brown, J., Lüthi, M. P., and Motyka, R. J.: Ice mélange dynamics and implications for terminus stability, Jakobshavn Isbræ, Greenland, Journal of Geophysical Research: Earth Surface, 115, https://doi.org/10.1029/2009JF001405, _eprint: https://onlinelibrary.wiley.com/doi/pdf/10.1029/2009JF001405, 2010.

Benn, D. I., Warren, C. R., and Mottram, R. H.: Calving processes and the dynamics of calving glaciers, Earth-Science Reviews, 82, 143–179, https://doi.org/10.1016/j.earscirev.2007.02.002, 2007.

Benn, D. I., Cowton, T., Todd, J., and Luckman, A.: Glacier Calving in Greenland, Current Climate Change Reports, 3, 282–290, https://doi.org/10.1007/s40641-017-0070-1, 2017.

Bondzio, J. H., Seroussi, H., Morlighem, M., Kleiner, T., Rückamp, M., Humbert, A., and Larour, E. Y.: Modelling calving front dynamics using a level-set method: application to Jakobshavn Isbræ, West Greenland, The Cryosphere, 10, 497–510, https://doi.org/10.5194/tc-10-497-2016, publisher: Copernicus GmbH, 2016.

Bondzio, J. H., Morlighem, M., Seroussi, H., Kleiner, T., Rückamp, M., Mouginot, J., Moon, T., Larour, E. Y., and Humbert, A.: The mechanisms behind Jakobshavn Isbræ's acceleration and mass loss: A 3-D thermomechanical model study, Geophysical Research Letters, 44, 6252–6260, https://doi.org/10.1002/2017GL073309, _eprint: https://onlinelibrary.wiley.com/doi/pdf/10.1002/2017GL073309, 2017.

Bondzio, J. H., Morlighem, M., Seroussi, H., Wood, M. H., and Mouginot, J.: Control of Ocean Temperature on Jakobshavn Isbræ's Present and Future Mass Loss, Geophysical Research Letters, 45, 12,912–12,921, https://doi.org/10.1029/2018GL079827, _eprint: https://onlinelibrary.wiley.com/doi/pdf/10.1029/2018GL079827, 2018.

Budd, W. F., Jenssen, D., and Smith, I. N.: A Three-Dimensional Time-Dependent Model of the West Antarctic Ice Sheet, Annals of Glaciology, 5, 29–36, https://doi.org/10.3189/1984AoG5-1-29-36, 1984.

Burton, J. C., Amundson, J. M., Cassotto, R., Kuo, C.-C., and Dennin, M.: Quantifying flow and stress in ice mélange, the world's largest granular material, Proceedings of the National Academy of Sciences, 115, 5105–5110, 2018.

Cassotto, R., Fahnestock, M., Amundson, J. M., Truffer, M., and Joughin, I.: Seasonal and interannual variations in ice melange and its impact on terminus stability, Jakobshavn Isbræ, Greenland, Journal of Glaciology, 61, 76–88, https://doi.org/10.3189/2015JoG13J235, publisher: Cambridge University Press, 2015.

Choi, Y., Morlighem, M., Wood, M., and Bondzio, J. H.: Comparison of four calving laws to model Greenland outlet glaciers, The Cryosphere, 12, 3735–3746, 2018.

Echelmeyer, K. and Harrison, W. D.: Jakobshavns Isbræ, West Greenland: Seasonal Variations in Velocity - or Lack Thereof, Journal of Glaciology, 36, 82–88, https://doi.org/10.3189/S0022143000005591, publisher: Cambridge University Press, 1990.

Ettema, J., van den Broeke, M. R., van Meijgaard, E., van de Berg, W. J., Bamber, J. L., Box, J. E., and Bales, R. C.: Higher surface mass balance of the Greenland ice sheet revealed by high-resolution climate modeling, Geophysical Research Letters, 36, https://doi.org/10.1029/2009GL038110, _eprint: https://onlinelibrary.wiley.com/doi/pdf/10.1029/2009GL038110, 2009.

Hanna, E., Huybrechts, P., Cappelen, J., Steffen, K., Bales, R. C., Burgess, E., McConnell, J. R., Peder Steffensen, J., Van den Broeke, M., Wake, L., Bigg, G., Griffiths, M., and Savas, D.: Greenland Ice Sheet surface mass balance 1870 to 2010 based

https://doi.org/10.5194/egusphere-2024-1435
Preprint. Discussion started: 10 June 2024

on Twentieth Century Reanalysis, and links with global climate forcing, Journal of Geophysical Research: Atmospheres, 116, https://doi.org/10.1029/2011JD016387, _eprint: https://onlinelibrary.wiley.com/doi/pdf/10.1029/2011JD016387, 2011.

Holland, D. M. and Jenkins, A.: Modeling Thermodynamic Ice–Ocean Interactions at the Base of an Ice Shelf, Journal of Physical Oceanography, 29, 1787–1800, https://doi.org/10.1175/1520-0485(1999)029<1787:MTIOIA>2.0.CO;2, publisher: American Meteorological Society Section: Journal of Physical Oceanography, 1999.

Holland, D. M., Thomas, R. H., de Young, B., Ribergaard, M. H., and Lyberth, B.: Acceleration of Jakobshavn Isbræ triggered by warm subsurface ocean waters, Nature Geoscience, 1, 659–664, https://doi.org/10.1038/ngeo316, number: 10 Publisher: Nature Publishing Group, 2008.

Howat, I. M., Negrete, A., and Smith, B. E.: The Greenland Ice Mapping Project (GIMP) land classification and surface elevation data sets, The Cryosphere, 8, 1509–1518, https://doi.org/10.5194/tc-8-1509-2014, publisher: Copernicus GmbH, 2014.

Joughin, I., Abdalati, W., and Fahnestock, M.: Large fluctuations in speed on Greenland's Jakobshavn Isbræ glacier, Nature, 432, 608–610, https://doi.org/10.1038/nature03130, number: 7017 Publisher: Nature Publishing Group, 2004.

Joughin, I., Howat, I., Alley, R. B., Ekstrom, G., Fahnestock, M., Moon, T., Nettles, M., Truffer, M., and Tsai, V. C.: Ice-front variation and tidewater behavior on Helheim and Kangerdlugssuaq Glaciers, Greenland, Journal of Geophysical Research: Earth Surface, 113, https://doi.org/10.1029/2007JF000837, _eprint: https://onlinelibrary.wiley.com/doi/pdf/10.1029/2007JF000837, 2008.

Joughin, I., Smith, B. E., and Medley, B.: Marine Ice Sheet Collapse Potentially Under Way for the Thwaites Glacier Basin, West Antarctica, Science, 344, 735–738, https://doi.org/10.1126/science.1249055, publisher: American Association for the Advancement of Science, 2014.

Joughin, I., Shean, D. E., Smith, B. E., and Floricioiu, D.: A decade of variability on Jakobshavn Isbræ: ocean temperatures pace speed through influence on mélange rigidity, The Cryosphere, 14, 211–227, https://doi.org/10.5194/tc-14-211-2020, publisher: Copernicus GmbH, 2020.

Kajanto, K., Seroussi, H., de Fleurian, B., and Nisancioglu, K. H.: Present day Jakobshavn Isbræ (West Greenland) close to the Holocene minimum extent, Quaternary Science Reviews, 246, 106 492, https://doi.org/https://doi.org/10.1016/j.quascirev.2020.106492, 2020.

Kajanto, K., Straneo, F., and Nisancioglu, K.: Impact of icebergs on the seasonal submarine melt of Sermeq Kujalleq, The Cryosphere, 17, 371–390, https://doi.org/10.5194/tc-17-371-2023, 2023.

Khazendar, A., Fenty, I. G., Carroll, D., Gardner, A., Lee, C. M., Fukumori, I., Wang, O., Zhang, H., Seroussi, H., Moller, D., Noël, B. P. Y., van den Broeke, M. R., Dinardo, S., and Willis, J.: Interruption of two decades of Jakobshavn Isbrae acceleration and thinning as regional ocean cools, Nature Geoscience, 12, 277–283, https://doi.org/10.1038/s41561-019-0329-3, number: 4 Publisher: Nature Publishing Group, 2019.

Korsgaard, N. J., Nuth, C., Khan, S. A., Kjeldsen, K. K., Bjørk, A. A., Schomacker, A., and Kjær, K. H.: Digital elevation model and orthophotographs of Greenland based on aerial photographs from 1978–1987, Scientific Data, 3, 160 032, https://doi.org/10.1038/sdata.2016.32, number: 1 Publisher: Nature Publishing Group, 2016.

Larour, E., Seroussi, H., Morlighem, M., and Rignot, E.: Continental scale, high order, high spatial resolution, ice sheet modeling using the Ice Sheet System Model (ISSM), Journal of Geophysical Research: Earth Surface, 117, https://doi.org/10.1029/2011JF002140, _eprint: https://onlinelibrary.wiley.com/doi/pdf/10.1029/2011JF002140, 2012.

Lee, R. W. and Schulson, E. M.: The Strength and Ductility of Ice Under Tension, Journal of Offshore Mechanics and Arctic Engineering, 110, 187–191, https://doi.org/10.1115/1.3257049, 1988.

Luckman, A., Benn, D. I., Cottier, F., Bevan, S., Nilsen, F., and Inall, M.: Calving rates at tidewater glaciers vary strongly with ocean temperature, Nature communications, 6, 8566, 2015.

https://doi.org/10.5194/egusphere-2024-1435
Preprint. Discussion started: 10 June 2024

MacAyeal, D. R.: Large-scale ice flow over a viscous basal sediment: Theory and application to ice stream B, Antarctica, Journal of Geophysical Research: Solid Earth, 94, 4071–4087, https://doi.org/10.1029/JB094iB04p04071, _eprint: https://onlinelibrary.wiley.com/doi/pdf/10.1029/JB094iB04p04071, 1989.

Morland, L. W. and Zainuddin, R.: Plane and Radial Ice-Shelf Flow with Prescribed Temperature Profile, in: Dynamics of the West Antarctic Ice Sheet, edited by Van der Veen, C. J. and Oerlemans, J., Glaciology and Quaternary Geology, pp. 117–140, Springer Netherlands, Dordrecht, https://doi.org/10.1007/978-94-009-3745-1_7, 1987.

Morlighem, M., Rignot, E., Seroussi, H., Larour, E., Ben Dhia, H., and Aubry, D.: Spatial patterns of basal drag inferred using control methods from a full-Stokes and simpler models for Pine Island Glacier, West Antarctica, Geophysical Research Letters, 37, https://doi.org/10.1029/2010GL043853, _eprint: https://onlinelibrary.wiley.com/doi/pdf/10.1029/2010GL043853, 2010.

Morlighem, M., Bondzio, J., Seroussi, H., Rignot, E., Larour, E., Humbert, A., and Rebuffi, S.: Modeling of Store Gletscher's calving dynamics, West Greenland, in response to ocean thermal forcing, Geophysical Research Letters, 43, 2659–2666, 2016.

Morlighem, M., Williams, C. N., Rignot, E., An, L., Arndt, J. E., Bamber, J. L., Catania, G., Chauché, N., Dowdeswell, J. A., Dorschel, B., Fenty, I., Hogan, K., Howat, I., Hubbard, A., Jakobsson, M., Jordan, T. M., Kjeldsen, K. K., Millan, R., Mayer, L., Mouginot, J., Noël, B. P. Y., O'Cofaigh, C., Palmer, S., Rysgaard, S., Seroussi, H., Siegert, M. J., Slabon, P., Straneo, F., van den Broeke, M. R., Weinrebe, W., Wood, M., and Zinglersen, K. B.: BedMachine v3: Complete Bed Topography and Ocean Bathymetry Mapping of Greenland From Multibeam Echo Sounding Combined With Mass Conservation, Geophysical Research Letters, 44, 11,051–11,061, https://doi.org/10.1002/2017GL074954, _eprint: https://onlinelibrary.wiley.com/doi/pdf/10.1002/2017GL074954, 2017.

Motyka, R. J., Truffer, M., Fahnestock, M., Mortensen, J., Rysgaard, S., and Howat, I.: Submarine melting of the 1985 Jakobshavn Isbræ floating tongue and the triggering of the current retreat, Journal of Geophysical Research: Earth Surface, 116, https://doi.org/10.1029/2009JF001632, _eprint: https://onlinelibrary.wiley.com/doi/pdf/10.1029/2009JF001632, 2011.

Mouginot, J., Rignot, E., Bjørk, A. A., van den Broeke, M., Millan, R., Morlighem, M., Noël, B., Scheuchl, B., and Wood, M.: Forty-six years of Greenland Ice Sheet mass balance from 1972 to 2018, Proceedings of the National Academy of Sciences, 116, 9239–9244, https://doi.org/10.1073/pnas.1904242116, publisher: Proceedings of the National Academy of Sciences, 2019.

Myers, P. G. and Ribergaard, M. H.: Warming of the Polar Water Layer in Disko Bay and Potential Impact on Jakobshavn Isbrae, Journal of Physical Oceanography, 43, 2629–2640, https://doi.org/10.1175/JPO-D-12-051.1, publisher: American Meteorological Society Section: Journal of Physical Oceanography, 2013.

Noël, B., van de Berg, W. J., van Meijgaard, E., Kuipers Munneke, P., van de Wal, R. S. W., and van den Broeke, M. R.: Evaluation of the updated regional climate model RACMO2.3: summer snowfall impact on the Greenland Ice Sheet, The Cryosphere, 9, 1831–1844, https://doi.org/10.5194/tc-9-1831-2015, publisher: Copernicus GmbH, 2015.

Petrovic, J. J.: Review Mechanical properties of ice and snow, Journal of Materials Science, 38, 1–6, https://doi.org/10.1023/A:1021134128038, 2003.

Pollard, D., DeConto, R. M., and Alley, R. B.: A continuum model (PSUMEL1) of ice mélange and its role during retreat of the Antarctic Ice Sheet, Geoscientific Model Development, 11, 5149–5172, 2018.

Rignot, E. and Mouginot, J.: Ice flow in Greenland for the International Polar Year 2008–2009, Geophysical Research Letters, 39, https://doi.org/10.1029/2012GL051634, _eprint: https://onlinelibrary.wiley.com/doi/pdf/10.1029/2012GL051634, 2012.

Rignot, E., Xu, Y., Menemenlis, D., Mouginot, J., Scheuchl, B., Li, X., Morlighem, M., Seroussi, H., den Broeke, M. v., Fenty, I., Cai, C., An, L., and Fleurian, B. d.: Modeling of ocean-induced ice melt rates of five west Greenland glaciers

https://doi.org/10.5194/egusphere-2024-1435
Preprint. Discussion started: 10 June 2024

over the past two decades, Geophysical Research Letters, 43, 6374–6382, https://doi.org/10.1002/2016GL068784, _eprint: https://onlinelibrary.wiley.com/doi/pdf/10.1002/2016GL068784, 2016.

Robel, A. A.: Thinning sea ice weakens buttressing force of iceberg mélange and promotes calving, Nature Communications, 8, 14 596, 2017.

Schlemm, T. and Levermann, A.: A simple parametrization of mélange buttressing for calving glaciers, The Cryosphere, 15, 531–545, 2021.

Schweinsberg, A. D., Briner, J. P., Miller, G. H., Bennike, O., and Thomas, E. K.: Local glaciation in West Greenland linked to North Atlantic Ocean circulation during the Holocene, Geology, 45, 195–198, https://doi.org/10.1130/G38114.1, 2017.

Seroussi, H., Morlighem, M., Rignot, E., Khazendar, A., Larour, E., and Mouginot, J.: Dependence of century-scale projections of the Greenland ice sheet on its thermal regime, Journal of Glaciology, 59, 1024–1034, https://doi.org/10.3189/2013JoG13J054, publisher: Cambridge University Press, 2013.

Seroussi, H., Morlighem, M., Larour, E., Rignot, E., and Khazendar, A.: Hydrostatic grounding line parameterization in ice sheet models, The Cryosphere, 8, 2075–2087, 2014.

Slater, D. A., Straneo, F., Das, S. B., Richards, C. G., Wagner, T. J. W., and Nienow, P. W.: Localized Plumes Drive Front-Wide Ocean Melting of A Greenlandic Tidewater Glacier, Geophysical Research Letters, 45, 12,350–12,358, https://doi.org/10.1029/2018GL080763, _eprint: https://onlinelibrary.wiley.com/doi/pdf/10.1029/2018GL080763, 2018.

Slater, D. A., Benn, D. I., Cowton, T. R., Bassis, J. N., and Todd, J. A.: Calving Multiplier Effect Controlled by Melt Undercut Geometry, Journal of Geophysical Research: Earth Surface, 126, e2021JF006 191, https://doi.org/10.1029/2021JF006191, _eprint: https://onlinelibrary.wiley.com/doi/pdf/10.1029/2021JF006191, 2021.

Smith, B., Fricker, H. A., Gardner, A. S., Medley, B., Nilsson, J., Paolo, F. S., Holschuh, N., Adusumilli, S., Brunt, K., Csatho, B., Harbeck, K., Markus, T., Neumann, T., Siegfried, M. R., and Zwally, H. J.: Pervasive ice sheet mass loss reflects competing ocean and atmosphere processes, Science, 368, 1239–1242, https://doi.org/10.1126/science.aaz5845, 2020.

Vaňková, I. and Holland, D. M.: A model of icebergs and sea ice in a joint continuum framework, Journal of Geophysical Research: Oceans, 122, 9110–9125, 2017.

Vaughan, D. G.: Relating the occurrence of crevasses to surface strain rates, Journal of Glaciology, 39, 255–266, 1993.

Xu, Y., Rignot, E., Fenty, I., Menemenlis, D., and Flexas, M. M.: Subaqueous melting of Store Glacier, west Greenland from three-dimensional, high-resolution numerical modeling and ocean observations, Geophys. Res. Lett., 40, 4648–4653, https://doi.org/10.1002/grl.50825, 2013.